

DEUTSCHES ELEKTRONEN – SYNCHROTRON

DESY 92-155
November 1992



Inclusive Production of Charged Pions, Kaons and Protons in $\Upsilon(4S)$ Decays

The ARGUS Collaboration

ISSN 0418-9833

NOTKESTRASSE 85 · D-2000 HAMBURG 52

DESY behält sich alle Rechte für den Fall der Schutzrechtserteilung und für die wirtschaftliche Verwertung der in diesem Bericht enthaltenen Informationen vor.

DESY reserves all rights for commercial use of information included in this report, especially in case of filing application for or grant of patents.

To be sure that your preprints are promptly included in the
HIGH ENERGY PHYSICS INDEX,
send them to (if possible by air mail):

DESY
Bibliothek
Notkestraße 85
W-2000 Hamburg 52
Germany

DESY-IfH
Bibliothek
Platanenallee 6
O-1615 Zeuthen
Germany

Inclusive Production of Charged Pions, Kaons and Protons in $\Upsilon(4S)$ Decays

The ARGUS Collaboration

H. Albrecht, H. I. Cronström¹, H. Ehrlichmann, T. Hamacher, R. P. Hofmann,
T. Kirchhoff, A. Neu, S. Nowak², M. Reidenbach, R. Reiner, H. Schröder, H. D. Schulz,
M. Walter³, R. Wurth
DESY, Hamburg, Germany

R. D. Appuhn, C. Hasat, E. Kolanoski, A. Lange, A. Lindner, R. Mankel, M. Schieber,
T. Siegmund, B. Spaan, H. Thurn, D. Töpfer, A. Walther, D. Wegener
Institut für Physik³, Universität Dortmund, Germany

M. Paulini, K. Reim, H. Wegener
Physikalisches Institut⁴, Universität Erlangen-Nürnberg, Germany

R. Mundt, T. Oest, W. Schmidt-Parzefall
II. Institut für Experimentalphysik, Universität Hamburg, Germany

W. Funk, J. Stieve, S. Werner
Institut für Hochenergiephysik⁵, Universität Heidelberg, Germany

K. Ehret, A. Hölischer, W. Hofmann, A. Hüpper, S. Khan, K. T. Knöpfle, J. Spengler
Max-Planck-Institut für Kernphysik, Heidelberg, Germany

D. I. Britton⁶, C. E. K. Charlesworth⁷, K. W. Edwards⁸, E. R. F. Hyatt⁹, H. Kapitza⁵,
P. Krüger⁹, D. B. MacFarlane⁶, P. M. Patel⁶, J. D. Prentice⁷, P. R. B. Saull⁶, S. C. Seidel⁷,
K. Trzarniudaki⁶, R. G. Van de Water⁷, T.-S. Yoon⁷
Institute of Particle Physics¹⁰, Canada

D. Reßing, M. Schmidler, M. Schneider, K. R. Schubert, K. Strahl, R. Waldi, S. Weseler
Institut für Experimentelle Kernphysik¹¹, Universität Karlsruhe, Germany

G. Kemel, P. Krizan, E. Kriznič, T. Podobnik, T. Živko
Institut J. Stefan and Oddelek za fiziko¹², Univerza v Ljubljani, Ljubljana, Slovenia

L. Jönsson
Institute of Physics¹³, University of Lund, Sweden

V. Balagura, I. Belyaev, M. Danilov, A. Drouotkov, A. Golutvin, I. Gorelov, G. Kostina,
V. Lubimov, P. Murat, P. Pakhlov, F. Batnikov, S. Semenov, V. Shibaev, V. Soloshenko,
I. Tichomirow, Yu. Zaitsev
Institute of Theoretical and Experimental Physics¹⁴, Moscow, Russia

¹ Supported in part by the Institute of Physics, University of Lund, Sweden

² DESY, DES Zeuthen

³ Supported by the German Bundesministerium für Forschung und Technologie, under contract number 064D061P.

⁴ Supported by the German Bundesministerium für Forschung und Technologie, under contract number 064ER12P.

⁵ Supported by the German Bundesministerium für Forschung und Technologie, under contract number 066HD21P.

⁶ McGill University, Montreal, Quebec, Canada.

⁷ University of Toronto, Toronto, Ontario, Canada.

⁸ Carleton University, Ottawa, Ontario, Canada.

⁹ Supported in part by the Walter C. Sumner Foundation.

¹⁰ Supported by the Natural Sciences and Engineering Research Council, Canada.

¹¹ Supported by the German Bundesministerium für Forschung und Technologie, under contract number 064KA17P.

¹² Supported by the Department of Science and Technology of the Republic of Slovenia and the Internazionalno Büro KLA, Ljubljana.

¹³ Supported by the Swedish Research Council.

¹⁴ Supported in part by the International Technology Center BINTEG, Moscow, Russia.

Abstract

Using the detector ARGUS at the e^+e^- storage ring DORIS II, we have investigated inclusive momentum spectra of charged pions, kaons, and protons from decays of the $\Upsilon(4S)$ meson. The kaon spectra have been measured in two independent ways, by coherently exploiting the detector's particle identification capabilities, and by detecting decays in-flight. The extracted mean multiplicities for charged hadrons are $7.17 \pm 0.05 \pm 0.14$ pions, $1.56 \pm 0.03 \pm 0.05$ kaons and $0.110 \pm 0.010 \pm 0.007$ protons per $\Upsilon(4S)$ decay, where pions and protons from K^0 and Λ decays have been subtracted.

1 Introduction

Our knowledge on B meson decays has greatly improved during the last decade. Besides the observation of $B^0\bar{B}^0$ mixing [1] which is an important ingredient in the framework of weak interaction in the quark sector, as many as 35% of exclusive B^0 , and 40% of exclusive B^+ decays have been experimentally established [2]. The remaining ones are for a large fraction high multiplicity decays, making exclusive analyses difficult due to a high combinatorial background. An alternative approach to the understanding of B meson decays is to study the hadronic decay products inclusively. Up to now, out of pions, kaons and protons only proton momentum spectra have been published by the CLEO [3] and ARGUS Collaborations [4], and the mean charged kaon multiplicity by CLEO [5,6]. There is, however, big interest in a precise determination of hadron spectra from B decays: they contain global information on B meson decay properties which have to be reproduced by any model trying to describe these decays. They are especially a testing ground for improved Monte Carlo generators which will be indispensable tools in planning experiments e.g. at future B meson factories or at hadron colliders. The more details of these spectra are known, the better is the estimation of backgrounds especially in regions where rare decays might become detectable.

The measurements described below have been obtained by using different techniques: The charged hadron spectra by coherently exploiting the detector's particle identification capabilities, and, for kaons, in a second, independent manner by observing decays in-flight.

The paper is organized as follows: First, we describe the analysis of charged pion, kaon and proton spectra based on the conventional tools for particle identification, namely specific energy loss dE/dx in the drift chamber gas, and velocity

measurement in the time-of-flight system. The results of this analysis will be discussed separately. Next, we describe the independent determination of the charged kaon spectrum based on decays in-flight and compare it to the first one.

2 Measurement of charged hadron spectra based on dE/dx and time-of-flight measurements

The determination of inclusive charged pion, kaon, and proton spectra from B meson decays presented here follows, as far as technique and algorithms are concerned, closely an analysis of inclusive hadron spectra from $\Upsilon(4S)$ decays and the neighbouring continuum, which has been published in a previous paper [7]. The technical details of the analysis have been discussed in the above publication but are briefly repeated here for the reader's convenience.

The data used for this analysis have been collected in 1985/86 with the detector ARGUS [8] at the e^+e^- storage ring DORIS II at DESY and comprise an integrated luminosity of 88.2 events/pb at the $\Upsilon(4S)$ energy, and 27.1 events/pb in the nearby continuum. This is only a minor fraction of the data available; for this data taking period, however, the drift chamber performance which plays the essential role for charged particle identification has been studied in great detail. Increasing the statistics would not improve the accuracy of results noticeably since systematic effects dominate.

Multihadron final states were selected by requiring at least three charged tracks from the interaction region. To eliminate beam wall and beam gas events as well as background from two-photon reactions we accept only events with

$$\sum |\vec{p}|/\sqrt{s} > 0.315 + \left(\sum p_z/\sqrt{s} \right)^2, \quad (1)$$

where \vec{p} is the particle's momentum vector, and p_z its component along the beam axis. The sums include the momenta of all photons as well as all charged particles which emerge from the interaction region or belong to a secondary vertex, with the exception of tracks belonging to a charged particle decaying in-flight. A more detailed description of this cut can be found in [9]. Radiative Bhabha events with converted photons are almost completely removed from the event sample by cutting on the sum E_{13} of the observed shower energies of the two particles with the largest momenta, and on an "isolated-track-angle" α , discriminating between topologies of radiative Bhabha and hadronic events. It is defined by the following procedure: Calculate first, for each charged or neutral particle, the smallest opening angle with respect to all other particles. This angle must be larger than 14° in order to also

reject doubly radiative Bhabha events. Then choose the largest one among these angles which results in nearly 180° for radiative Bhabha events, whereas less than 90° is characteristic for $g\bar{q}$ and $B\bar{B}$ events. The cut applied was [9]:

$$E_{13}/\sqrt{s} - 0.53 \cdot \cos \alpha \leq 0.371. \quad (2)$$

After these cuts we are left with 87,475 events in the continuum, and 353,544 events at the $\Upsilon(4S)$ energy. From these events, charged tracks were selected which originate in a volume of 1.5 cm radial, and 5 cm longitudinal (i.e. along the beam direction) extension from the nominal interaction point. The momentum vector had to fulfil $p_{\perp} > 0.05 \text{ GeV}/c$ and $|\cos \theta| < 0.85$, both with respect to the beam axis.

Charged particles can be identified using information from two detector components: the main drift chamber, providing dE/dx information, and the barrel time-of-flight (TOF) counters which surround the drift chamber at a radial distance of 95 cm from the beam axis.

The dE/dx samples from all wires hit are corrected for space charge effects and averaged, discarding the highest 30% and lowest 10% of the values measured [10]. The track cuts ensure that at least 10 hits contribute to this "truncated mean".

The time-of-flight measured for an individual particle is corrected for a pulse height dependent time shift [11]. It is only used as an additional information for tracks with $|\cos \theta| < 0.60$, if a TOF counter can be uniquely assigned to the track.

Probability distributions in the specific energy loss, $f_1(dE/dx|\vec{p})$, and time of flight, $g_1(\text{TOF}|\vec{p})$, have been precisely parametrized for the selected data, using clean samples of electrons (from radiative Bhabha events), pions (from K^0 decays), kaons (from D^0 decays through the decay chain $D^{*+} \rightarrow D^0\pi^+$, $D^0 \rightarrow K^-\pi^+$) and protons (from Λ decays). For the dE/dx distributions, this has been done in the accessible range of momentum p and in dependence on the run periods, polar angle θ , number of hits in the drift chamber, electric charge, and momentum uncertainty. For the TOF-distributions, it was done in dependence on run periods, polar angle θ , individual TOF-counter, light yield in the TOF-counter, and momentum uncertainty. The spectra for charged pions, kaons and protons have been obtained from a maximum likelihood fit of a sum of these distributions to all selected tracks in the multi-dimensional space of all variables on which the distributions depend, using as free parameters the numbers of π^\pm , K^\pm , $p + \bar{p}$, e^\pm , and μ^\pm in each momentum bin [12]. For the proton distribution at momenta below $1.2 \text{ GeV}/c$, instead of $p + \bar{p}$, two times the antiprotons were used in order to avoid any problems with protons which originate from secondary interactions. Since the TOF and dE/dx distributions for pions and leptons, especially muons have considerable overlaps, the numbers of electrons and muons are further constrained to fit predetermined distributions

$h_e(p)$ and $h_\mu(p)$ within their systematical errors. For electrons, h_e is a smooth function which is obtained from data in the regions where electrons can be identified, as shown in fig.1 for $\sqrt{s} = 10.58$ GeV. This function leads to the same spectrum of electrons measured at momenta above 0.8 GeV/c, if the electrons are identified with the help of the ARGUS shower counter system. The distribution h_μ has been determined from the Monte Carlo using the model by Wirbel, Stech and Bauer [13] for semileptonic decays of B and D mesons. Continuum events were modelled by the LUND 6.2 Monte Carlo program [14]. The Monte Carlo predictions from these programs are consistent with the spectrum of muons measured at momenta above 1.4 GeV/c where they are identified with the help of the ARGUS muon chambers. A systematical error σ_μ of the distribution h_μ of 20% has been used to include model variations and branching ratio uncertainties. The corresponding error for the electrons σ_e has been found to be 5% considering the results of the fit to the electron data (fig.1). The complete likelihood function to be maximized for each momentum interval of charged tracks thus becomes

$$L(n_e, n_K, n_p, n_\pi, n_\mu) = \prod_{i=1}^N \left(\sum_{j=\pi, K, p, \mu} \frac{n_j}{\sum n_k} \cdot f_j((dE/dx)_i, \vec{p}_i) \cdot g_j(\text{TOF}_i, \vec{p}_i) \right) \cdot \exp \left(- \frac{[n_\mu - h_\mu(p)]^2}{2\sigma_\mu^2(p)} - \frac{[n_e - h_e(p)]^2}{2\sigma_e^2(p)} \right) \cdot \exp \left(- \sum n_k \right) \cdot \left(\sum n_k \right)^N \quad (3)$$

where p_i is the momentum measured in the drift chamber, N is the total number of observed charged tracks in the momentum interval, and the n_j are the numbers of particles of type j to be fitted. The last two factors reflect the Poisson distribution of the total number of tracks. This fit is performed in narrow intervals of the momentum extrapolated, for each hadron separately, to the interaction point from that one measured in the drift chamber. Details can be found in [12]. In fig.2 we have superimposed the results of the fit to the observed dE/dx and TOF distributions in one momentum interval.

Since the acceptance for tracks from secondary vertices is different from that for tracks from the interaction region, the decay products of K^0 and Λ were treated separately: Using momentum distributions for K^0 mesons [15] and Λ baryons [4] obtained from our data, we subtract all pions and (anti-) protons from the decays of these particles which have not yet been removed by the cut on the track origin. The uncertainty in the K^0 multiplicity of 7% leads to a systematic error in the π^\pm multiplicity of 0.6%.

To determine particle spectra from $\Upsilon(4S)$ decays, the underlying continuum has to be subtracted, whereby the different amounts of resonant vector meson states from the radiative process $e^+e^- \rightarrow \gamma V$ at both energies have been taken into ac-

count:

$$\frac{1}{\sigma_{\text{dir}}} \frac{d\sigma_{\text{dir}}(p)}{dp} = a \cdot \frac{1}{\sigma_{\text{cont}}} \frac{d\sigma_{\text{cont}}(p)}{dp} - a' \cdot \frac{1}{\sigma_{\text{off}}} \frac{d\sigma_{\text{off}}(p)}{dp} + a'' \cdot \frac{1}{\sigma_{\text{res}}} \frac{d\sigma_{\text{res}}(p)}{dp} \quad (4)$$

Here, the subscript "dir" refers to direct resonance decays, "on" to all hadronic events at the energy of the $\Upsilon(4S)$ resonance, "off" to all events in the continuum, and "res" (resonances) to the correction for the resonances with $J^{PC} = 1^{--}$ in the radiative tail of the continuum: the continuum spectra to be subtracted were scaled by a factor $s_{\text{off}}/s_{\text{on}}$. On the other hand, the continuum contains resonances like the $\Upsilon(3S)$, $\Upsilon(2S)$, $\Upsilon(1S)$ and other 1^{--} states with lower mass whose contributions do not scale like $1/s$; this deviation from the $1/s$ -scaling was taken into account by the factor a'' which was determined to be 3.8% by using the Lund Monte Carlo program (version 6.2 [14]) slightly modified to include the contribution of vector meson resonances to the initial-photon spectrum [16]. Using $\sigma_{\text{cont}} = \sigma_{\text{off}} \cdot s_{\text{off}}/s_{\text{on}}$ and σ_{res} from Monte Carlo, we obtain

$$\begin{aligned} \sigma_{\text{dir}} &= \sigma_{\text{on}} - \sigma_{\text{cont}} + \sigma_{\text{res}} \\ a &= \sigma_{\text{on}}/\sigma_{\text{dir}} \\ a' &= \sigma_{\text{cont}}/\sigma_{\text{dir}} \\ a'' &= \sigma_{\text{res}}/\sigma_{\text{dir}} \end{aligned} \quad (5)$$

In order to calculate the acceptance, $\Upsilon(4S)$ decays were modelled through a Monte Carlo simulation. All events were subsequently passed through a simulation of the detector ARGUS [17], and processed with the same reconstruction and analysis programs as the data.

The acceptance corrected momentum spectra for decays of the $\Upsilon(4S)$ resonance, where pions and protons from K^0 and Λ decays have been subtracted, are shown in fig.3 for pions, in fig.4 for kaons and in fig.5 for protons. The spectra are listed numerically in tables 1,2 and 4. In order to compare with other experiments, we quote for pions and protons also the numbers including K^0 and Λ decay products.

The error bars in all figures correspond to statistical and momentum dependent systematical errors added in quadrature. The latter include the uncertainties in the dE/dx and TOF parametrizations for charged particles, and of our Monte Carlo simulation; another part of systematic uncertainty comes from the errors on the constants needed to determine a, a', a'' for the continuum subtraction. A momentum independent overall uncertainty, which amounts to $\pm 1.1\%$ in all spectra, is not included in the error bars.

In fig.3, 4 and 5 our results are compared to the predictions of the Monte Carlo generator LUND 7.3 [18]. Large discrepancies are evident as well at low momenta, where fragmentation processes dominate, as at higher momenta, where low multiplicity decays prevail. These clearly call for a more elaborate model of B decays.

Especially high momentum pions from $b \rightarrow u$ transitions are clearly overestimated by the LUND model.

Average multiplicities for all charged hadrons have been obtained by integrating the momentum distributions of figs. 3-5, where pions and protons from K^0 and Λ decays have been subtracted or included. The results are compared to the LUND prediction, and to the result from CLEO in table 5. The systematic errors include the uncertainty in the extrapolation to the full momentum range.

3 Measurement of the charged kaon momentum spectrum based on reconstruction of decays in-flight

For charged kaons, a measurement of the momentum spectrum independent of particle identification tools such as dE/dx and TOF is possible, namely by exploiting the kaons' decays in-flight: Due to a value of $c \cdot \tau = 370.9$ cm, roughly 10% of the charged kaons decay inside the detector volume. Since both, the kaon and at least one of its charged decay particles, must be recognized, the sensitive volume for the kaon decay vertex reconstruction is restricted to the central part of the drift chamber. The total efficiency amounts to 4 % for kaons with momenta of 300 MeV/c ($\beta_K = 0.5$) and drops to 0.4% at 2 GeV/c ($\beta_K = 0.97$). The advantage of this method is the clean signature given by the decay vertex lying well inside the drift chamber where background from converted photons and hadronic interactions in the detector material is negligible. The total data sample was used corresponding to an integrated luminosity of 234 events/pb at the $\Upsilon(4S)$ resonance energy, and 92 events/pb in the neighbouring continuum. The data selection was performed starting with the same cuts against beam-gas background and Bhabha events as in the previous analysis.

Most of the kaons decay into one charged plus neutral particles. The branching ratio for these decays is 94%, dominated by the channels $K^+ \rightarrow \mu^+ \nu_\mu$ (63.51%) and $K^+ \rightarrow \pi^+ \pi^0$ (21.17%). The decay into three charged pions does not noticeably improve the statistical accuracy and was not investigated here. In the data, the decays under study show up as two equally charged tracks with a kink ("charged- Vee^0 -topology") in the drift chamber. The kaon must originate in the primary interaction volume. The two charged tracks are sufficient to identify the kaon decay in-flight.

In the region of high kaon momenta, the statistical error is dominated by the

continuum subtraction. To reduce this effect, jet like (i.e. continuum) events were rejected by requiring the second Fox-Wolfgram moment to obey $H_2 < 0.4$. This cut removes about 1% of $\Upsilon(4S)$ decays, and about 28% of continuum events. The invariant mass of the unobserved neutral decay products, as calculated from the charged particles' four-momenta, must be greater than $(p_K - p_\mu)^2 > -0.1$ GeV² to suppress background from particles which undergo hadronic interactions with the drift chamber gas or drift chamber wires*. This selection yields a sample of 12,029 kaon candidates in the $\Upsilon(4S)$ data and 2,526 in the continuum. The momentum spectrum of kaons from $\Upsilon(4S)$ decays was obtained after subtracting the continuum contribution. Additional background sources are pion decays $\pi^\pm \rightarrow \mu^\pm \nu_\mu$, hadronic interactions and converted photons. These background contributions have been estimated using a Monte Carlo simulation. They amount to roughly $5 \cdot 10^{-3}$ of the kaon rate and have been subtracted as well. A study of the measured invariant mass distribution $(p_K - p_\mu)^2$ allows an independent estimate of this background which is less than $2.7 \cdot 10^{-3}$.

The efficiency to reconstruct a kaon decay has been calculated from a Monte Carlo simulation. It depends on the decay angle and the number of drift chamber hits found per track. Distributions of these quantities are well reproduced in the simulation. The errors include systematic uncertainties of the following origins: Fake pion subtraction, Fox-Wolfgram moment cut, momentum dependent vertex and track reconstruction efficiencies, and continuum subtraction. There are, in addition, overall uncertainties on the scale which amount to 10% due to the vertex and track reconstruction efficiencies as far as these are momentum independent, and 8.6% from the momentum independent part of the continuum subtraction.

The charged kaon momentum spectrum from this analysis of kaons decaying in-flight is numerically displayed in Table 3. Integrating the spectrum yields a kaon multiplicity per $\Upsilon(4S)$ decay of $1.41 \pm 0.09 \pm 0.20$. There is good agreement between the kaon spectra of both methods, as shown in fig. 6.

4 Summary

To summarize, we have measured momentum spectra for charged pions, kaons, and protons from $\Upsilon(4S)$ decays, covering the kinematical range up to the highest possible momenta. The kaon distributions have been determined using two independent methods which lead to consistent results. None of these spectra shows any distinct structure indicating that there are no strong contributions from two-body decays.

*The muon mass was used for the charged decay particle here. Due to the small difference to the π^\pm mass this doesn't affect the calculated mass significantly.

The measured meson multiplicity reflects the dominance of $b \rightarrow c$ - mediated B meson decays. These measurements represent an essential input for improved Monte Carlo generators which are needed for e.g. future B meson factories.

5 Acknowledgments

It is a pleasure to thank U. Djuanda, E. Konrad, E. Michel, and W. Reinsch for their competent technical help in running the experiment and processing the data. We thank Dr. H. Niesemann, B. Sarau, and the DORIS group for the excellent operation of the storage ring. The visiting groups wish to thank the DESY directorate for the continuous support and kind hospitality extended to them.

References

- [1] H. Albrecht et al. (ARGUS), Phys. Lett. B192 (1987) 245.
- [2] M. Danilov, in Proceedings of the Joint International Lepton-Photon Symposium & Europhysics Conference on High Energy Physics, Geneva, 1991: edited by S. Hegarty, K. Porter, E. Quercigh, World Scientific, Singapore, 1992
- [3] G. Crawford et al. (CLEO), Phys. Rev. D46 (1992) 752.
- [4] H. Albrecht et al. (ARGUS), Z. Phys. C42 (1989) 519.
- [5] A. Brody et al. (CLEO), Phys. Rev. Lett. 48 (1982) 1070
- [6] M. S. Alam et al. (CLEO), Phys. Rev. Lett. 58 (1987) 1814.
- [7] H. Albrecht et al. (ARGUS), Z. Phys. C44 (1989) 547.
- [8] H. Albrecht et al. (ARGUS), Nucl. Instr. Meth. A275 (1989) 1.
- [9] H. Albrecht et al. (ARGUS), Z. Phys. C54 (1992) 13.
- [10] M. Danilov et al., Nucl. Instr. Meth. A217 (1983) 153.
- [11] R. Heller et al., Nucl. Instr. Meth. A235 (1985) 26.
- [12] W. Funk, Dissertation, IHEP-HD/91-3, Heidelberg 1991.
- [13] M. Wirbel, B. Stech, M. Bauer, Z. Phys. C29 (1985) 637.
- [14] T. Sjöstrand, Comp. Phys. Comm. 27(1982) 243; 30 (1986) 347.
- [15] H. I. Cronström, Ph.D. Thesis, University of Lund, LUNFD6/(NFFL-7066) 1991.
- [16] F. A. Berends, R. Kleiss, Nucl. Phys. B178 (1981) 141.
- [17] H. Gennow, Internal Report DESY F15-85-02.
- [18] T. Sjöstrand et al., "The Lund Monte Carlo Programs", CERN Program Library (1989).

Table 1: $\frac{1}{\sigma} \frac{d\sigma(\pi^\pm)}{dp}$ from $\Upsilon(4S)$ -decays, scale uncertainty = 1.1%

p-interval [GeV/c]	without K_0^0 and Λ decay particles	with K_0^0 and Λ decay particles
0.075-0.100	8.104 ± 0.255 ± 0.332	9.356 ± 0.255 ± 0.383
0.100-0.125	9.439 ± 0.273 ± 0.239	11.121 ± 0.273 ± 0.281
0.125-0.150	9.967 ± 0.283 ± 0.385	12.036 ± 0.283 ± 0.465
0.150-0.175	11.238 ± 0.310 ± 0.376	13.575 ± 0.310 ± 0.455
0.175-0.200	11.217 ± 0.335 ± 0.307	13.772 ± 0.335 ± 0.377
0.200-0.225	12.208 ± 0.351 ± 0.337	14.786 ± 0.351 ± 0.408
0.225-0.250	12.153 ± 0.365 ± 0.292	14.514 ± 0.365 ± 0.348
0.250-0.275	12.148 ± 0.369 ± 0.293	14.268 ± 0.369 ± 0.344
0.275-0.300	12.194 ± 0.367 ± 0.366	14.179 ± 0.367 ± 0.426
0.300-0.325	11.811 ± 0.363 ± 0.248	13.658 ± 0.363 ± 0.286
0.325-0.350	11.650 ± 0.358 ± 0.325	13.367 ± 0.358 ± 0.373
0.350-0.375	11.010 ± 0.351 ± 0.286	12.649 ± 0.351 ± 0.328
0.375-0.400	10.085 ± 0.344 ± 0.232	11.562 ± 0.344 ± 0.266
0.400-0.425	10.160 ± 0.335 ± 0.188	11.514 ± 0.335 ± 0.213
0.425-0.450	9.378 ± 0.325 ± 0.182	10.650 ± 0.325 ± 0.207
0.450-0.475	8.957 ± 0.317 ± 0.231	10.112 ± 0.317 ± 0.261
0.475-0.500	8.198 ± 0.307 ± 0.145	9.271 ± 0.307 ± 0.164
0.500-0.525	7.801 ± 0.301 ± 0.262	8.762 ± 0.301 ± 0.294
0.525-0.550	6.806 ± 0.293 ± 0.103	7.645 ± 0.293 ± 0.116
0.550-0.575	6.175 ± 0.284 ± 0.056	6.957 ± 0.284 ± 0.063
0.575-0.600	6.222 ± 0.273 ± 0.151	6.924 ± 0.273 ± 0.168
0.600-0.625	5.380 ± 0.267 ± 0.073	6.021 ± 0.267 ± 0.082
0.625-0.650	5.309 ± 0.258 ± 0.091	5.877 ± 0.258 ± 0.100
0.650-0.675	5.096 ± 0.251 ± 0.105	5.636 ± 0.251 ± 0.116
0.675-0.700	4.193 ± 0.247 ± 0.129	4.671 ± 0.247 ± 0.144
0.700-0.725	3.882 ± 0.238 ± 0.215	4.315 ± 0.238 ± 0.239
0.725-0.750	3.933 ± 0.232 ± 0.134	4.341 ± 0.232 ± 0.147
0.750-0.775	3.785 ± 0.224 ± 0.148	4.157 ± 0.224 ± 0.162
0.800-0.800	3.370 ± 0.222 ± 0.116	3.689 ± 0.222 ± 0.127
0.900-1.000	1.861 ± 0.105 ± 0.072	2.042 ± 0.105 ± 0.079
1.000-1.100	1.160 ± 0.105 ± 0.089	1.280 ± 0.105 ± 0.099
1.100-1.200	0.811 ± 0.110 ± 0.089	0.891 ± 0.110 ± 0.098
1.200-1.300	0.623 ± 0.115 ± 0.136	0.676 ± 0.115 ± 0.148
1.300-1.400	0.433 ± 0.110 ± 0.064	0.473 ± 0.110 ± 0.070
1.400-1.500	0.454 ± 0.096 ± 0.075	0.477 ± 0.096 ± 0.079
1.500-1.600	0.208 ± 0.080 ± 0.072	0.223 ± 0.080 ± 0.077
1.600-1.700	0.141 ± 0.071 ± 0.058	0.150 ± 0.071 ± 0.061
1.700-1.800	0.175 ± 0.064 ± 0.043	0.181 ± 0.064 ± 0.045
1.800-1.900	0.102 ± 0.059 ± 0.028	0.105 ± 0.059 ± 0.029
1.900-2.000	0.090 ± 0.053 ± 0.029	0.091 ± 0.053 ± 0.030
2.000-2.100	0.123 ± 0.049 ± 0.029	0.125 ± 0.049 ± 0.030
2.100-2.200	0.066 ± 0.044 ± 0.033	0.067 ± 0.044 ± 0.033
2.200-2.300	0.140 ± 0.038 ± 0.017	0.140 ± 0.038 ± 0.017
2.300-2.400	0.010 ± 0.035 ± 0.027	0.010 ± 0.035 ± 0.027
2.400-2.500	0.021 ± 0.031 ± 0.034	0.021 ± 0.031 ± 0.034
2.500-2.600	0.026 ± 0.027 ± 0.014	0.026 ± 0.027 ± 0.014
2.600-2.700	-0.015 ± 0.025 ± 0.025	-0.015 ± 0.025 ± 0.025
2.700-2.800	-0.011 ± 0.024 ± 0.016	-0.011 ± 0.024 ± 0.016

Table 2: $\frac{1}{\sigma} \frac{d\sigma(K^\pm)}{dp}$ from $\Upsilon(4S)$ -decays, scale uncertainty = 1.1%

p-interval [GeV/c]	
0.175-0.200	0.678 ± 0.081 ± 0.097
0.200-0.225	1.032 ± 0.086 ± 0.095
0.225-0.250	1.240 ± 0.087 ± 0.108
0.250-0.275	1.386 ± 0.087 ± 0.071
0.275-0.300	1.423 ± 0.093 ± 0.126
0.300-0.325	1.501 ± 0.092 ± 0.071
0.325-0.350	1.611 ± 0.094 ± 0.096
0.350-0.375	1.893 ± 0.098 ± 0.084
0.375-0.400	1.834 ± 0.100 ± 0.057
0.400-0.425	2.083 ± 0.099 ± 0.075
0.425-0.450	2.009 ± 0.103 ± 0.068
0.450-0.475	2.000 ± 0.103 ± 0.056
0.475-0.500	2.130 ± 0.104 ± 0.084
0.500-0.525	1.952 ± 0.106 ± 0.094
0.525-0.550	1.887 ± 0.107 ± 0.086
0.550-0.575	1.822 ± 0.108 ± 0.086
0.575-0.600	1.809 ± 0.108 ± 0.072
0.600-0.625	1.904 ± 0.109 ± 0.071
0.625-0.650	1.732 ± 0.111 ± 0.086
0.650-0.675	1.571 ± 0.113 ± 0.063
0.675-0.700	1.521 ± 0.112 ± 0.060
0.700-0.725	1.405 ± 0.113 ± 0.133
0.725-0.750	1.392 ± 0.114 ± 0.091
0.750-0.775	1.379 ± 0.112 ± 0.156
0.775-0.800	1.200 ± 0.118 ± 0.115
0.800-0.900	0.917 ± 0.060 ± 0.051
0.900-1.000	0.957 ± 0.066 ± 0.054
1.000-1.100	0.659 ± 0.079 ± 0.092
1.100-1.200	0.403 ± 0.094 ± 0.063
1.200-1.300	0.572 ± 0.103 ± 0.131
1.300-1.400	0.535 ± 0.101 ± 0.029
1.400-1.500	0.208 ± 0.084 ± 0.074
1.500-1.600	0.312 ± 0.067 ± 0.042
1.600-1.700	0.160 ± 0.056 ± 0.019
1.700-1.800	0.124 ± 0.049 ± 0.024
1.800-1.900	0.013 ± 0.044 ± 0.030
1.900-2.000	0.065 ± 0.039 ± 0.011
2.000-2.100	-0.062 ± 0.039 ± 0.021
2.100-2.200	-0.026 ± 0.037 ± 0.010
2.200-2.300	0.024 ± 0.035 ± 0.027
2.300-2.400	-0.021 ± 0.033 ± 0.023
2.400-2.500	0.014 ± 0.036 ± 0.023
2.500-2.600	-0.032 ± 0.033 ± 0.023
2.600-2.700	0.040 ± 0.034 ± 0.011
2.700-2.800	0.046 ± 0.037 ± 0.022

Table 4: $\frac{1}{\sigma} \frac{d\sigma(p\bar{p})}{d\Omega}$ from $\Upsilon(4S)$ -decays, scale uncertainty = 1.1%

p-interval [GeV/c]	without Λ decay particles	with Λ decay particles
0.300-0.400	0.117 ± 0.025 ± 0.012	0.172 ± 0.025 ± 0.017
0.400-0.500	0.115 ± 0.032 ± 0.002	0.198 ± 0.032 ± 0.003
0.500-0.600	0.201 ± 0.033 ± 0.005	0.274 ± 0.033 ± 0.007
0.600-0.700	0.120 ± 0.035 ± 0.008	0.190 ± 0.035 ± 0.013
0.700-0.800	0.125 ± 0.034 ± 0.010	0.175 ± 0.034 ± 0.013
0.800-0.900	0.068 ± 0.033 ± 0.011	0.124 ± 0.033 ± 0.016
0.900-1.000	0.112 ± 0.031 ± 0.001	0.136 ± 0.031 ± 0.001
1.000-1.100	0.054 ± 0.031 ± 0.009	0.077 ± 0.031 ± 0.012
1.100-1.200	0.060 ± 0.030 ± 0.003	0.072 ± 0.030 ± 0.003
1.200-1.300	-0.012 ± 0.022 ± 0.019	-0.004 ± 0.022 ± 0.019
1.300-1.400	0.010 ± 0.022 ± 0.029	0.014 ± 0.022 ± 0.040
1.400-1.500	-0.021 ± 0.023 ± 0.013	-0.018 ± 0.023 ± 0.013
1.500-1.600	-0.021 ± 0.025 ± 0.014	-0.020 ± 0.025 ± 0.014
1.600-1.700	-0.011 ± 0.027 ± 0.013	-0.010 ± 0.027 ± 0.013
1.700-1.800	-0.016 ± 0.029 ± 0.014	-0.016 ± 0.029 ± 0.014
1.800-1.900	0.034 ± 0.032 ± 0.016	0.034 ± 0.032 ± 0.016
1.900-2.000	-0.020 ± 0.033 ± 0.027	-0.020 ± 0.033 ± 0.027
2.000-2.100	0.031 ± 0.038 ± 0.015	0.031 ± 0.038 ± 0.015
2.100-2.200	-0.003 ± 0.038 ± 0.025	-0.003 ± 0.038 ± 0.025

Table 3: $\frac{1}{\sigma} \frac{d\sigma(K^\pm)}{d\Omega}$ from $\Upsilon(4S)$ -decays (kaons decaying in-flight), scale uncertainty = 14.1%

0.200-0.300	1.21 ± 0.09 ± 0.13
0.300-0.400	1.71 ± 0.12 ± 0.17
0.400-0.500	1.75 ± 0.15 ± 0.17
0.500-0.600	2.01 ± 0.18 ± 0.20
0.600-0.700	1.45 ± 0.18 ± 0.14
0.700-0.800	1.20 ± 0.18 ± 0.12
0.800-0.900	0.98 ± 0.18 ± 0.09
0.900-1.000	0.97 ± 0.20 ± 0.09
1.000-1.100	0.64 ± 0.17 ± 0.06
1.100-1.200	0.13 ± 0.17 ± 0.06
1.200-1.300	0.56 ± 0.16 ± 0.05
1.300-1.400	0.23 ± 0.17 ± 0.03
1.400-1.500	0.09 ± 0.13 ± 0.02
1.500-1.600	0.15 ± 0.15 ± 0.02
1.600-1.700	0.09 ± 0.13 ± 0.01
1.700-1.800	-0.11 ± 0.17 ± 0.03
1.800-1.900	0.01 ± 0.15 ± 0.02
1.900-2.000	-0.07 ± 0.09 ± 0.01
2.000-2.100	-0.03 ± 0.09 ± 0.01
2.100-2.200	0.19 ± 0.19 ± 0.02
2.200-2.300	0.27 ± 0.29 ± 0.04
2.300-2.400	0.15 ± 0.19 ± 0.01
2.400-2.500	-0.11 ± 0.16 ± 0.01
2.500-2.600	-0.06 ± 0.14 ± 0.01
2.600-2.700	0.04 ± 0.09 ± 0.00
2.700-2.800	0.02 ± 0.04 ± 0.02

Table 5: π^\pm , K^\pm and p, \bar{p} multiplicities obtained with ARGUS by exploiting the detector's particle identification capabilities and for kaons decaying in-flight, compared to the Monte Carlo generator and to the results from CLEO. Contributions from K^0 and Λ decays to these multiplicities have been subtracted or included. The value for the kaons is the weighted average of the result of the two methods of $1.56 \pm 0.03 \pm 0.05$ and $1.41 \pm 0.09 \pm 0.20$, respectively

	ARGUS	CLEO	LUND 7.3
π^\pm not from K^0, Λ	7.17 ± 0.05 ± 0.14	-	7.08
π^\pm incl. K^0, Λ	8.21 ± 0.05 ± 0.16	-	7.91
K^\pm	1.55 ± 0.03 ± 0.05	1.94 ± 0.47 [5] 1.70 ± 0.23 [6]	1.44
p, \bar{p} not from Λ	0.110 ± 0.010 ± 0.007	0.112 ± 0.012 ± 0.010 [3]	0.029
p, \bar{p} incl. Λ	0.160 ± 0.010 ± 0.010	0.160 ± 0.010 ± 0.006 [3]	0.031

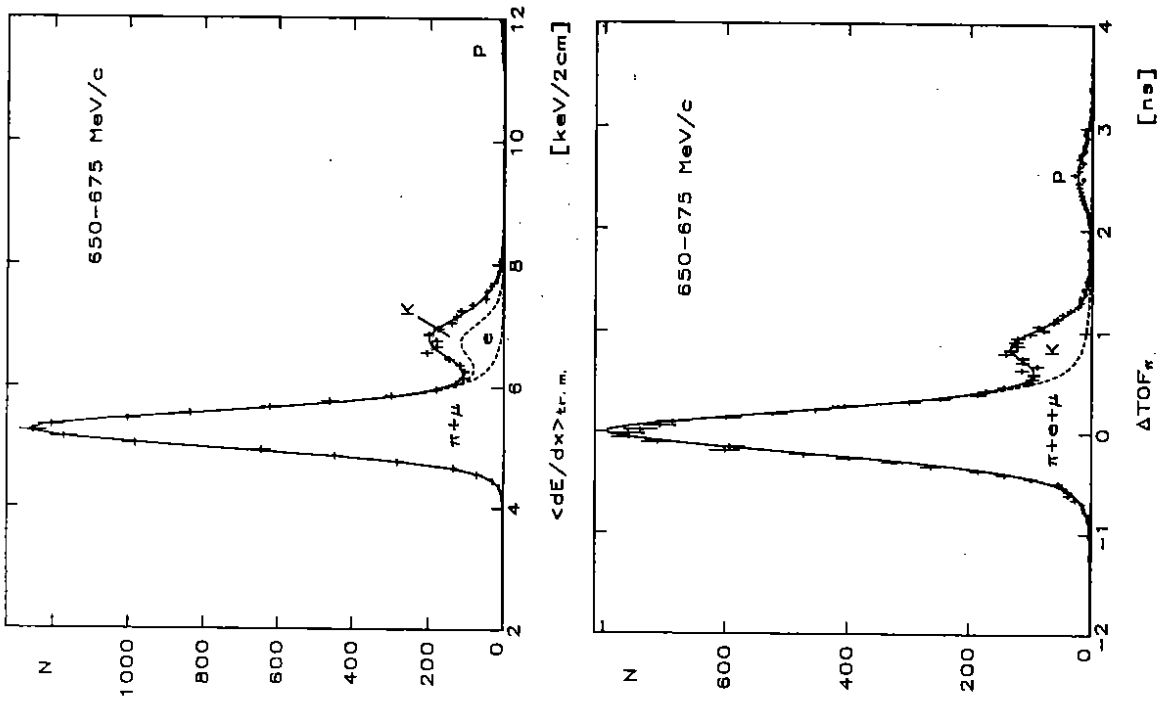


Figure 2: Statistical particle separation: (a) The dE/dx distribution is shown together with the results of a fit for $0.65\text{GeV}/c < p < 0.675\text{GeV}/c$. Protons are still clearly separated in this momentum region. (b) The time-of-flight distribution for the same momentum interval.

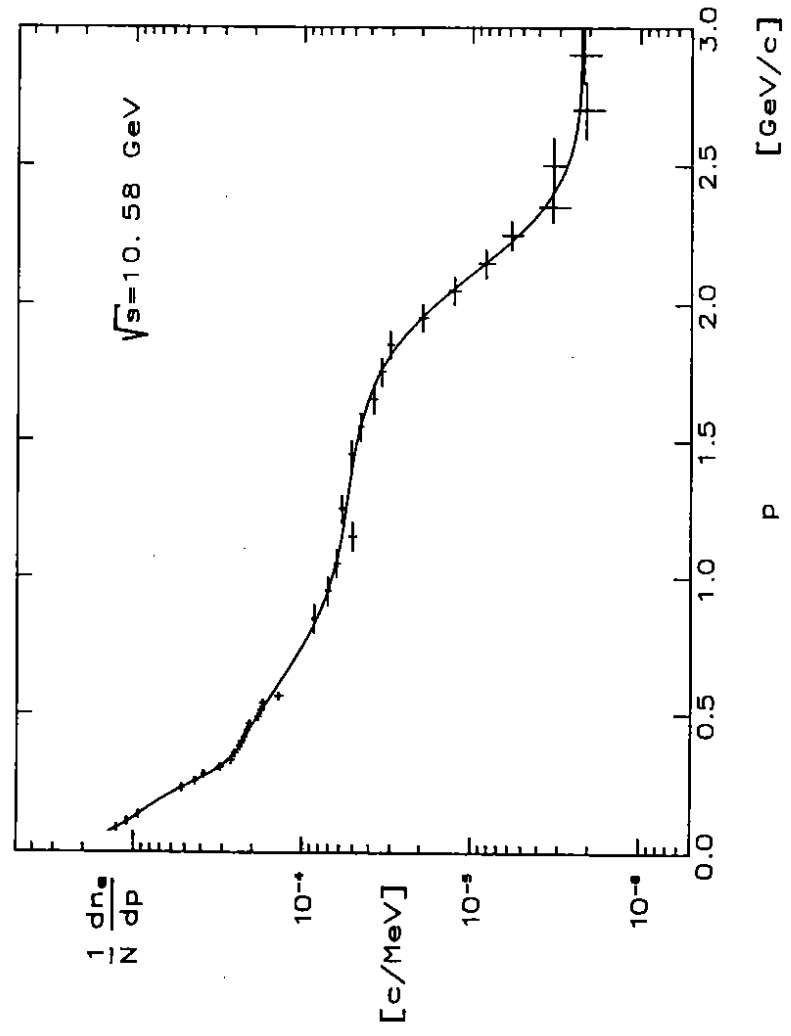


Figure 1: Fit result and interpolation function for the electrons at $\sqrt{s} = 10.58\text{ GeV}$. To account for electrons in the charged hadron data in momentum regions where they can't be separated, their contribution is constrained to fit this interpolation function.

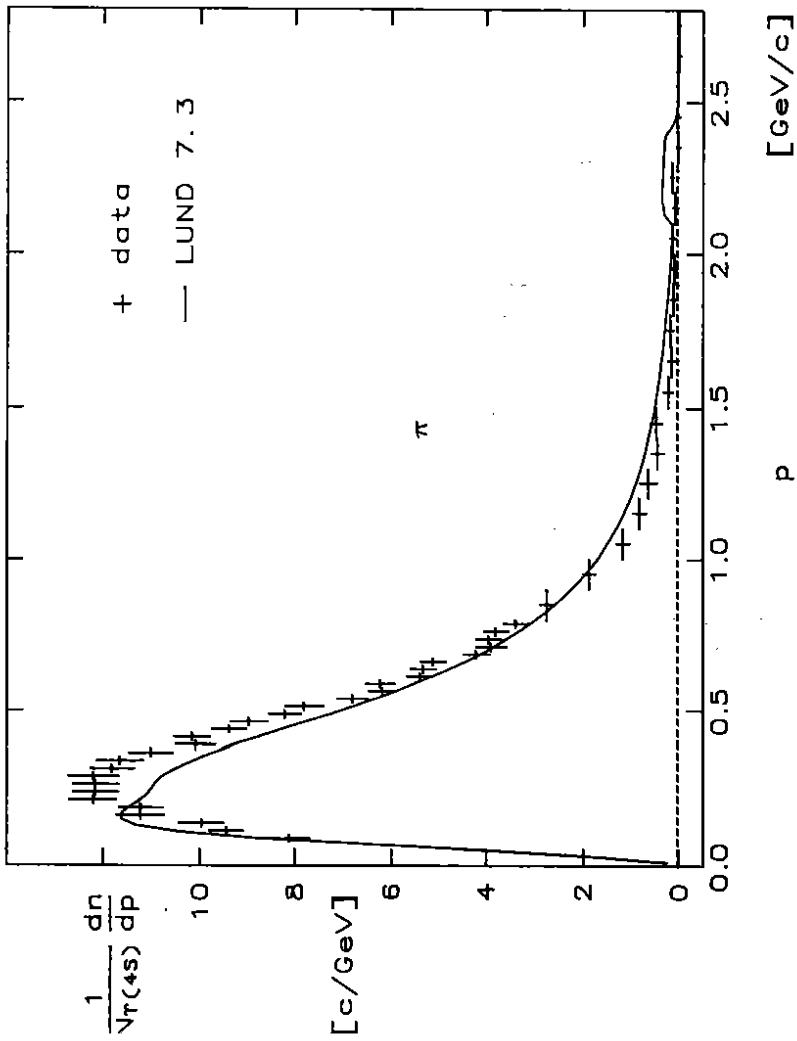


Figure 3: The pion momentum spectrum obtained from dE/dx and TOF analysis after acceptance correction compared to the LUND 7.3 prediction. Contributions from K^0 and Λ decays have been subtracted.

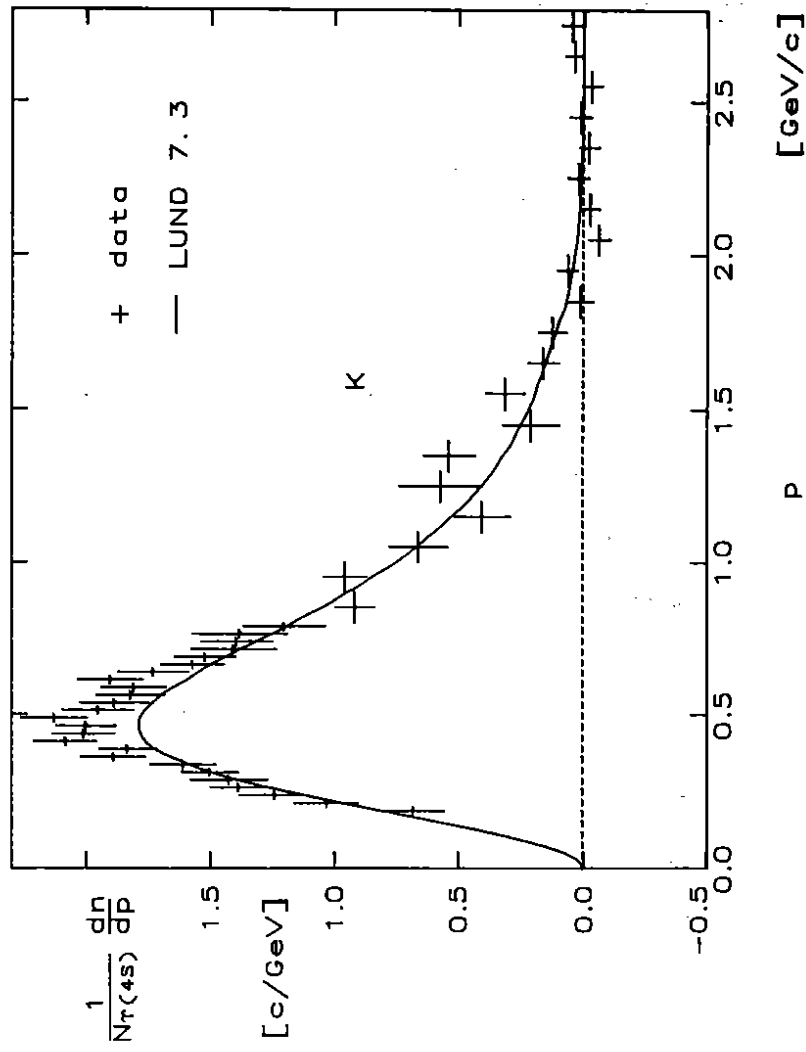


Figure 4: The kaon momentum spectrum obtained from dE/dx and TOF analysis after acceptance correction compared to the LUND 7.3 prediction.

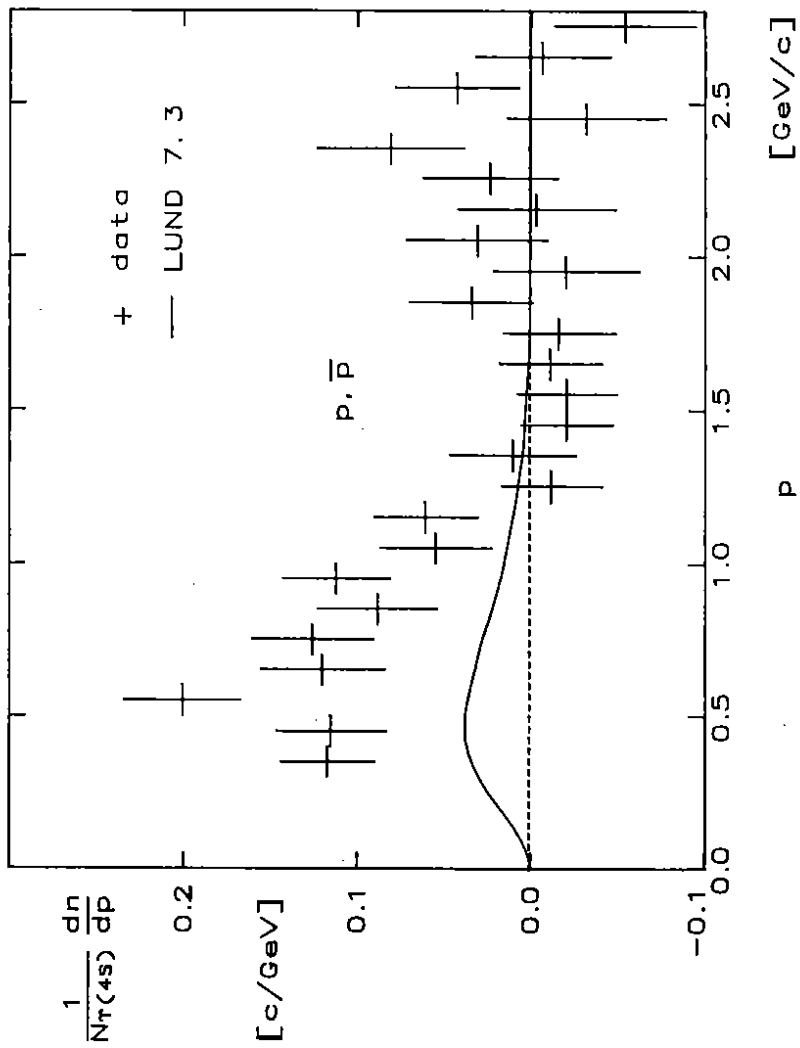


Figure 5: The proton momentum spectrum obtained from dE/dx and TOF analysis after acceptance correction compared to the LUND 7.3 prediction. Contributions from Λ decays have been subtracted.

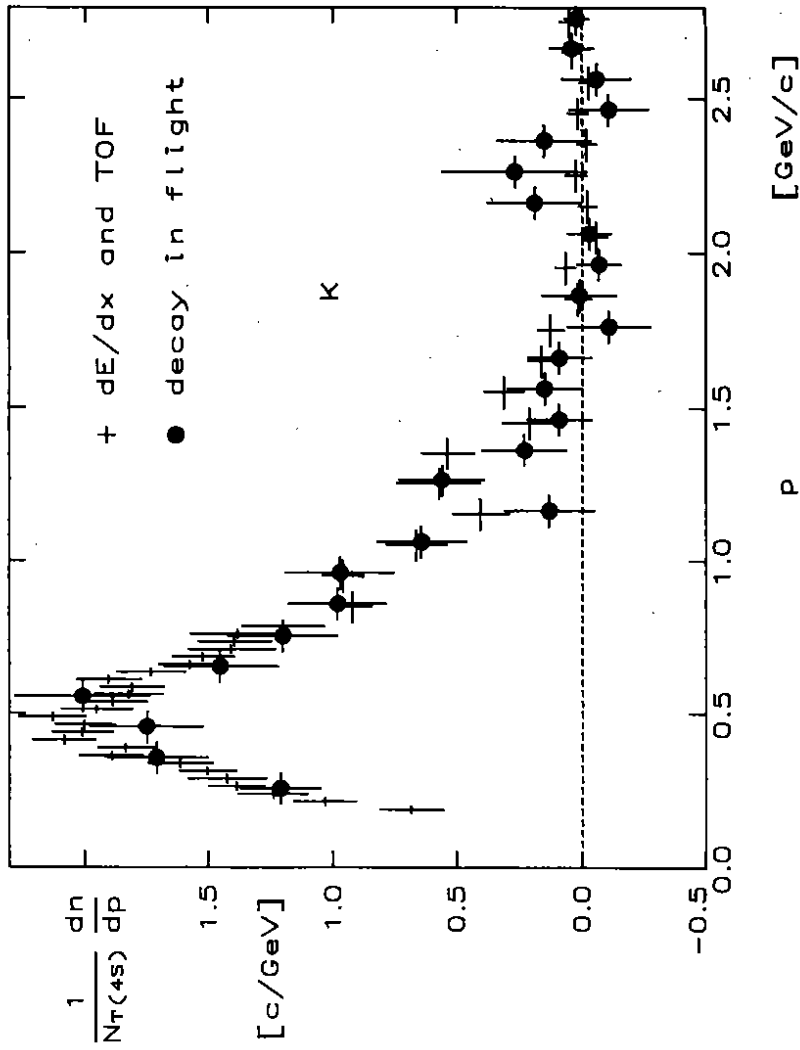


Figure 6: Comparison of kaon momentum spectra as obtained by dE/dx and TOF analysis, and by the analysis of decays in-flight.